Progress in Renewable Energies Offshore – Guedes Soares (Ed.)
© 2016 Taylor & Francis Group, London, ISBN 978-1-138-62627-0

Assessing the utility and effectiveness of the IEC standards for wave energy resource characterisation

V. Ramos
Centre for Ocean Energy Research, Maynooth University, Maynooth, Ireland

R. Carballo
Hydraulic Engineering, University of Santiago de Compostela, EPS, Lugo, Spain

John V. Ringwood
Centre for Ocean Energy Research, Maynooth University, Maynooth, Ireland

ABSTRACT: Over the next decades, wave energy aims to become a commercially viable source of energy. For this purpose, a complete understanding of the wave resource characterisation is needed. In this context, the International Electrotechnical Commission (IEC) has developed a technical specification for the assessment of the wave resource, *IEC-TS 62600-101: Marine energy-Wave, tidal and other water current converters-Part 101: Wave energy resource assessment and characterisation* (IEC-TS). IEC-TS classifies resource assessment studies into three different categories: reconnaissance, feasibility and design. The requirements for the model setup (mesh resolution, boundary conditions) and the effort (validation process, computational times) vary considerably from one class to the other. Accordingly, the main goal of this work is to explore this methodology using the Irish West coast as a case study. Overall, it was found that the methodology proposed performs well, offering a detailed characterisation of the resource; however, with the aim of making the technical specification more manageable, some aspects related to the validation and model setup procedures may be revisited for future editions.

1 INTRODUCTION

During last years, marine energy has aroused great interest in both the academic and industrial communities, due to its large energy potential (Bahaj 2011, Carballo, Iglesias, & Castro 2009, Ramos, Carballo, Alvarez, Sanchez, & Iglesias 2014, Ramos & Iglesias 2013, Veigas, Carballo, & Iglesias 2014). Among them, wave energy appears as a promising, virtually untapped, alternative (Iglesias & Carballo 2011), with multitude of potential locations around the to be exploited (Rusu & Soares 2012, Iglesias, Lopez, Carballo, Castro, Fraguela, & Frigaard 2009, Iglesias & Carballo 2010). However, for wave energy to become a commercially-viable energy source, several issues such as resource estimation, environmental impacts and technology development must be addressed in detail (Iglesias & Carballo 2014, Carballo & Iglesias 2013). Among them, the level of uncertainty in the assessment of the wave energy resource stands out (Farrell, Donoghue, & Morrissey 2015). So far, wave resource characterisation was mainly carried out based on a relatively small number of sea states, which were propagated towards the shore by means of spectral wave models (Iglesias, Lopez, Carballo, Castro, Fraguela, & Frigaard 2009, Lopez, Veigas, & Iglesias 2015, Veigas, Lopez, & Iglesias 2014), with the aim of determining the average wave power over a coastal region. However, for a better understanding of the practical resource, the assessment should cover a large portion of the available energy (at least 90%) (Carballo & Iglesias 2012) and also take into consideration the seasonal variability of the resource (Carballo, Sanchez, Ramos, Fraguela, & Iglesias 2015b, Carballo, Sanchez, Ramos, Fraguela, & Iglesias 2015a, Neill & Hashemi 2013).

On these grounds, the International Electrotechnical Commission (IEC) has recently put forward a series of recommendations to develop a standard methodology with the aim of ensuring consistency and accuracy in wave resource characterisation: *IEC-TS 62600-101: Marine energy Wave, tidal and other water current converters-Part 101: Wave energy resource assessment and characterisation* (from now on referred as IEC-TS) [2]. The IEC-TS classifies the resource assessment studies into three different categories: reconnaissance, feasibility and design, with the notation of Class 1, 2 and 3, respectively. Class 1 is intended to obtain a first approximation of the wave energy resource

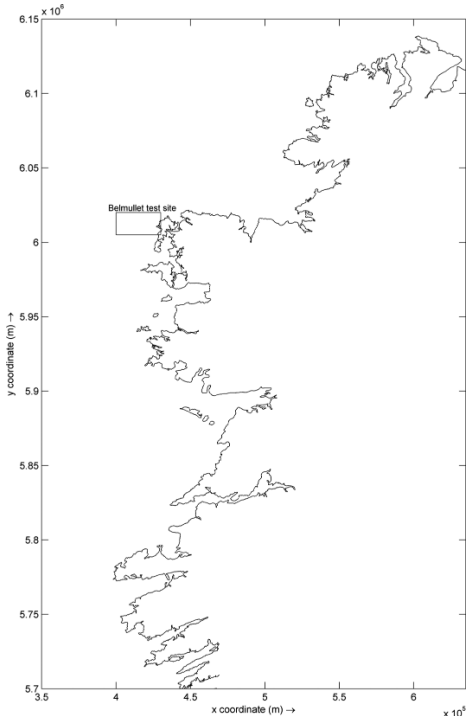

Figure 1. Location of Irish West coast and Belmullet test site.

over a relatively large area of seascape and would be the first resource assessment conducted in a region. Class 2 assessments are focused on smaller areas being suitable for refinement of the results obtained from the Class 1 assessments. Finally, Class 3 assessments are used to obtain a detailed characterisation in a relatively small area of seascape for the final project design stage, producing results with a low degree of uncertainty.

From the modelling standpoint, the implications on the wave model setup process vary considerably depending on the class considered, especially in terms of the boundary condition data and mesh resolution requirements, with the result that the level of effort required for the modelling process varies significantly from one class to another. For these reasons, the objective of the study reported in this paper is two-fold: (i) to compare the three different classes of the IEC-TS in terms of uncertainty in the resource assessment and the effort required for the model setup (mesh resolution, wave data and computational times) and (ii) to provide feedback into the IEC-TS with the aim of offering both practical recommendations to the users and future edits to be considered during IEC-TS maintenance.

For this purpose, the Irish West coast, which presents one of the most energetic wave climates in the world (Tiron, Gallagher, Gleeson, Dias, & Mc-Grath 2015) was used as case study. Due to its large energetic potential, the Sustainable Energy Authority of Ireland (SEAI) is intended to develop the Belmullet Wave Energy Test Site, which will be located in Annagh Head, West of Belmullet in Co. Mayo, Rep. of Ireland (Figure 1).

This paper is structured as follows: Section 2 presents the main characteristics of the IEC-TS. Section 3 presents the materials and methods used in this investigation. Section 4 shows the results obtained during validation and wave resource characterisation. Section 5, presents a discussion regarding the most relevant aspects of the IEC-TS. Finally, conclusions are drawn in section 6.

2 IEC 62600-101 TS: MARINE ENERGY—WAVE, TIDAL AND OTHER WATER CURRENT CONVERTERS-PART 101: WAVE ENERGY RESOURCE ASSESSMENT AND CHARACTERISATION

IEC-TS aims to set a series of standards related to the measurement, modelling, analysis and reporting of the wave energy resource, and the linkages between these activities. In this section, the main characteristics of the IEC-TS regarding the modelling aspects will be presented. For further details in other aspects, such as data collection and data analysis, the readers are referred to the IEC-TS document (International Electrotechnical Commision, IEC 2014).

2.1 *IEC 62600-101: wave model setup*

As mentioned before, the technical specification divides the resource assessment studies into three different categories: reconnaissance, feasibility and design, with the notation of Class 1, 2 and 3, respectively. The main characteristics of each class are summarised in Table 1.

Independently of the class considered, the numerical model used to estimate the resource should produce a minimum of ten years of sea state data, which shall be generated with a minimum frequency of one data set every three hours. However, for each class, the model setup requirements vary considerably, especially regarding the physical

Table 1. Classes of resource assessment.

Class	Description	Uncertainty wave resource	Long-shore extent (km)
Class 1	Reconnaissance	High	> 300
Class 2	Feasibility	Medium	20–500
Class 3	Design	Low	< 25

Table 2. IEC-TS model setup recommendations.

Component	Class 1	Class 2	Class 3
Physical processes			
Wind-wave growth	●	●	●
Whitecapping	●	●	●
Quadruplet interactions	●	●	●
Wave breaking	○	●	●
Bottom friction	○	●	●
Triad interactions	●	●	●
Diffraction	●	●	●
Refraction	●	●	●
Wave reflections	●	●	●
Wave-current interactions	●	●	●
Numerics			
Parametric wave model	○	★	★
2*nd* generation spectral wave model	○	○	★
3*rd* generation spectral wave model	✻	✻	✻
Mild-slope wave model	○	○	○
Spherical coordinates	●	○	○
Non-stationary solution	○	○	○
Min. spatial resolution	5 km	500 m	50 m
Min. temporal resolution	3 hrs	3 hrs	1 hr
Min. num. wave frequencies	25	25	25
Min. num. azimuthal direction	24	24	24
Boundary Conditions			
Parametric boundary	○	★	★
Hybrid boundary	○	○	★
Spectral boundary	✻	✻	✻

● Mandatory ✻ Recommended ○ Accpetable ★ Not permitted

processes that must be considered and the spatial and temporal resolutions.

Regarding the wave boundary conditions, the IEC-TS classifies them into three different types: (i) parametric boundaries, which are based on a predefined spectral shape (e.g. JONSWAP, Pierson-Moscowitz, Bretschneider) defined by characteristic parameters such as significant wave height, H_{m0}, peak period, T_p and mean wave direction θ_m, (ii) hybrid boundary conditions, characterised by wave spectrum with parametric directional parameters and (iii) spectral boundaries defined by a directional wave spectrum. These boundary conditions should be defined using either: (i) physically recorded meteocean data, (ii) historical data obtained from a more extensive numerical model or (iii) a combination of the first two options. In all cases, the data should cover a period of at least ten years, with a data return rate greater than 70% for the case of the recorded meteocean data.

The main characteristics for the model setup process of each class are summarised in Table 2:

2.2 *IEC 62600-101: wave model validation*

The IEC-TS has developed its own validation procedure, with the aim of offering robustness and accuracy to this process. Overall, the validation data set should cover a period of one year, with a monthly return rate of recorded data exceeding 70%. Then, this data set must be used to construct an omni-directional $H_{m0} - T_e$ scatter table showing the proportional frequency of occurrence of different sea states. Finally, the validation coverage will be defined as the sum of the proportional frequency of occurrence of the represented scatter table cells. A cell in the scatter table will be considered to be representative as long as it contains a minimum number of validation data points. All these requirements are shown in Table 3.

The model error is evaluated by considering the data in each scatter table cell, and overall. For each represented cell, the normalized error, e_p, between measured and modelled values of a parameter, p, must be calculated as:

$$e_p = \begin{bmatrix} |(p_{M1} - p_{D1})|/p_{D1} \\ \vdots \\ |(p_{Mn} - p_{Dn})|/p_{Dn} \end{bmatrix} \quad (1)$$

where, p_{Mk}, and, p_{Dk}, are values at coincident time-steps t_k for $k = 1...n$ of the modelled and measured parameter, respectively. For each cell, the normalised error must be separated into a systematic error, $\mu_{ij}(e_p)$, and a random error, $\sigma_{ij}(e_p)$. The systematic error, or bias, is defined as the mean of errors in cell, (i, j), (Eq. 2), whereas the random error is represented by the standard deviation of the errors in cell, (i, j), (Eq. 3):

$$\mu_{ij} = \frac{1}{N}\sum_{k=1}^{N} e_{p_{ij}} \quad (2)$$

$$\sigma_{ij} = \sqrt{\frac{1}{N-1}\sum_{k=1}^{N}(e_{p_{ij}} - \mu_{ij})^2} \quad (3)$$

The significance of the systematic and random errors at each cell may be related to their influence on the estimation of the energy resource. Therefore,

Table 3. IEC-TS validation recommendations.

	Class 1	Class 2	Class 3
Data coverage			
Min. num. of cell data points	3	5	5
Min. coverage by validation data	90%	90%	95%
Max. acceptable $b_{(ep)}$			
Sig. wave height, H_{m0}	10%	5%	2%
Energy period, T_e	10%	5%	2%
Omni-directional wave power, J	25%	12%	5%
Dir. of max dir. resolved power, θ_{Jmax}	–	10°	5°
Spectral width, $\in_0$	–	12%	5%
Directionality coefficient, d	–	12%	5%
Max. acceptable $\sigma(e_p)$			
Sig. wave height, H_{m0}	15%	10%	7%
Energy period, T_e	15%	10%	7%
Omni-directional wave power, J	35%	25%	20%
Dir. of max dir. resolved power, θ_{Jmax}	–	15°	10°
Spectral width, $\in_0$	–	25%	15%
Directionality coefficient, d	–	25%	15%

for each cell (i, j), the product of the proportional frequency of occurrence, f_{ij}, and mean incident wave power, J_{ij}, gives a strong indication of any error and should constitute the basis for computing the weighting factor, w_{ij}:

$$w_{ij} = J_{ij} f_{ij} \tag{4}$$

For those cells (i, j), where the minimum number of validation data points is not reached (Table 3), f_{ij}, must be set to zero. Furthermore, if a specific WEC technology is being considered the weighting factor, w_{ij}, may be redefined taking into consideration the capture length, L_{ij}, associated with each cell:

$$w_{ij} = L_{ij} J_{ij} f_{ij} \tag{5}$$

In any case, the weighting matrix shall be normalised such its sum is equal to one:

$$\widehat{w_{ij}} = \frac{w_{ij}}{\sum_{i,j} w_{ij}} \tag{6}$$

Therefore, the weighted mean random error, $\sigma(e_p)$, and the weighted systematic error, $b(e_p)$, can be calculated as the sum of the element-wise product of the normalised weighting matrix and the random and systematic error matrices, respectively:

$$\sigma(e_p) = \sum_{i,j} \widehat{w_{ij}} \sigma_{ij} \tag{7}$$

$$b(e_p) = \sum_{i,j} \widehat{w_{ij}} \mu_{ij} \tag{8}$$

Table 3 summarises, for each class of resource assessment, the maximum acceptable weighted mean systematic and random errors for every validation parameter.

3 MATERIALS AND METHODS

3.1 *SWAN numerical wave model*

With the aim of determining the wave energy resource in the area of study, the spectral wave model SWAN (Delft University of Techonology 2014) (Simulating WAves Nearshore) was used. SWAN is an open source third-generation wave model developed by Delft University of Technology, which has been successfully applied in a large number of studies dealing with wave resource assessment (Bento, Martinho, & Soares 2015, Silva, Bento, Martinho, & Soares 2015, Soares, Bento, Gonçalves, Silva, & Martinho 2014, Iglesias & Carballo 2009). SWAN calculates the development of a sea state based on the wave action density $N(\sigma, \theta)$, since it is conserved in the presence of ambient currents $\vec{U}$, whereas energy density $E(\sigma, \theta)$ is not (Delft University of Techonology 2014). The wave action density is defined as the variance density E divided by the relative frequency (σ), ($N = E/\sigma$). The evolution of the action density is governed by the action balance equation, which can be expressed as:

$$\frac{\partial N}{\partial t} + \nabla_{\vec{x}} \cdot [(\vec{C}_g) + \vec{U})N] + \frac{\partial c_\sigma N}{\partial \sigma} + \frac{\partial c_\theta N}{\partial \theta} = \frac{S_{tot}}{\sigma} \tag{9}$$

The left-hand side represents the kinematic part of the equation. $\frac{\partial N}{\partial t}$, denotes the evolution of the action density as function of the time. $\nabla_{\vec{x}} \cdot [(\vec{C}_g) + \vec{U})N]$, represents the propagation of wave energy with the group velocity $\vec{c}_g = \partial\sigma / \partial\vec{k}$ following from the dispersion relation $\sigma^2 = g|\vec{k}|\tanh(|\vec{k}|d)$ where $\vec{k}$ is the wave number vector and d the water depth. $\frac{\partial c_\sigma N}{\partial \sigma}$, stands for the effect of shifting of the radian frequency due to variations in depth and mean currents. Finally, $\frac{\partial c_\theta N}{\partial \theta}$, represents the effects of the depth and current induced refraction. The quantities c_σ and c_θ stand for the propagation velocities in spectral space (σ, θ).

Regarding the right-hand side of eq. (9), S_{tot} represents the source/sink term, which takes into

account the physical processes of generation, dissipation and nonlinear wave-wave interactions. S_{tot} can be expressed as follows:

$$S_{tot} = S_{in} + S_{nl3} + S_{nl4} + S_{ds,w} + S_{ds,b} + S_{ds,br} \quad (10)$$

where S_{in} denotes the wave growth by wind; S_{nl3} and S_{nl4} refer to the nonlinear transfer of wave energy through three-wave (triads) and four-wave interactions (quadruplets), respectively; and finally $S_{ds,w}$, $S_{ds,b}$ and $S_{ds,br}$ represent the wave decay due to white-capping, bottom friction and depth-induced wave breaking, respectively (Delft University of Techonology 2014, der Westhuysen AJ. 2002, Booij N 1999).

Finally, SWAN computes the components of wave power per meter of wave front, $J(Wm^{-1})$ from the full wave spectrum, according to the following expressions:

$$J_x = \rho g \int_0^{2\pi} \int_0^{\infty} c_g(\sigma,d) E(\sigma,\theta) \cos(\theta) d\sigma d\theta \quad (11)$$

$$J_y = \rho g \int_0^{2\pi} \int_0^{\infty} c_g(\sigma,d) E(\sigma,\theta) \sin(\theta) d\sigma d\theta \quad (12)$$

where ρ is the water density, g is the acceleration due to gravity and x, y are the grid coordinate directions. Therefore, the wave power is calculated as:

$$J = \sqrt{(J_x^2 + J_y^2)} \quad (13)$$

3.2 *Wave model implementation*

Three different spectral wave models, corresponding with the three different classes proposed by the IEC-TS, were implemented in the area of study. The model corresponding with class 1 (MI) spans an area approximately of 90000 km^2, implemented in a structured grid (cartesian) with a resolution of 1000 x 1000 m (Figure 2), which extends from (x = 329594 m, y = 5684380 m) to (x = 602594 m, y = 6153381 m). With respect to the class 2 model (MII), it covers an area approximately of 18000 km^2, implemented again in a cartesian grid with a resolution of 500 x 500 m (Figure 3), which extends from (x = 362000 m, y = 5910000 m) to (x = 540000 m, y = 6065000 m). Finally, for the class 3 model (MIII), the computational domain covers roughly the area occupied by the Belmullet test site (approx. 1480 km^2), extending from (x = 398000 m, y = 5982000 m) to (x = 450000 m, y = 6036000 m). In this case an unstructured mesh was used, which allowed for a much better representation of the coastlines and the areas around the islands than the cartesian grids, and also provided the opportunity to concentrate the mesh resolution in areas of specific interest (i.e. the validation points). The unstructured mesh contains approximately

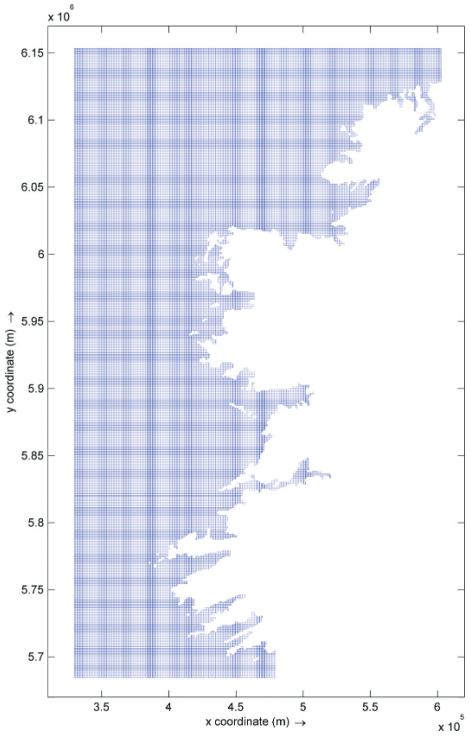

Figure 2. MI structured computational grid.

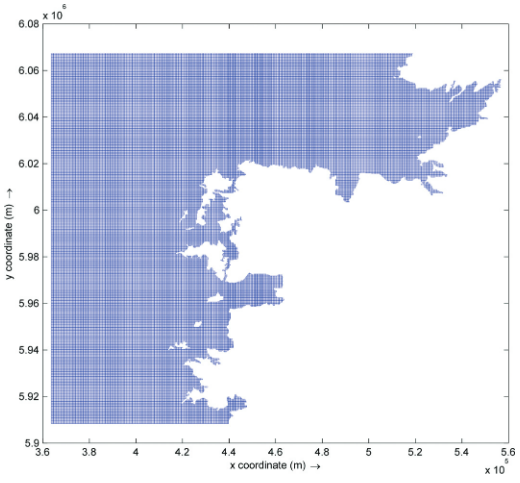

Figure 3. MII structured computational grid.

80000 cells of triangular shape, with a grid size ranging from 85 m to 700 m (Figure 4).

The bathymetry data for the region of study was obtained from the British Oceanographic Data Center (BODC) through the General Bathymetric Chart of the Oceans (GEBCO) gridded bathymetric data sets. Then, these data sets were interpolated

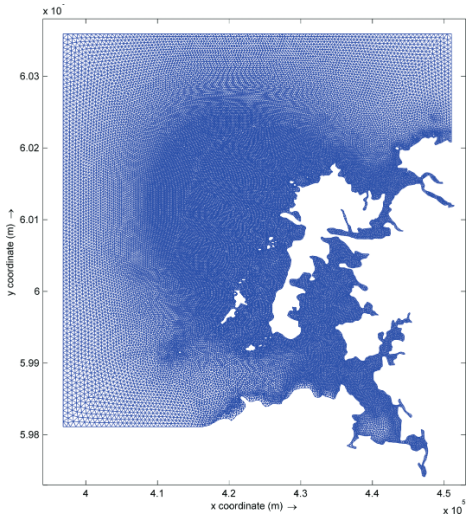

Figure 4. MIII unstructured computational grid.

according to the resolution of the different models (MI, MII and MIII).

The wave boundary conditions used for the model implementation were obtained from the Spanish State Port Authority (Puertos del Estado) through the SIMAR-44 data sets. The SIMAR-44 data sets consist of a hindcast obtained through numerical modelling by coupling both a high-resolution atmospheric model (REMO) and a wave model (WAM). The REMO model, which was forced with global reanalysis data from the National Center for Environmental Prediction (NCEP), was used to produce a high-resolution atmospheric data sets, which were used to force the third generation spectral wave model WAM. The WAM model solves as well as SWAN does the action balance equation (Eq. 9). The model was implemented on a computational grid, which covers all the North Atlantic with a resolution of 30' (lat) x 30' (lon) without assuming any particular spectral shape and producing results with a frequency of 1 hr.

Therefore, for the present study, wave data covering a period of ten years from 01/01/2005 to 31/12/2014 with a time interval of 1 hr, were extracted from the SIMAR-44 data sets in order to produce the wave boundary conditions for the models MI and MII. As mentioned in Section II, the characteristics of the wave boundary conditions depend on the class considered. On these grounds, for the class 1 model (MI), the parametrised sea state approach was used, with the sea state conditions limited to the significant wave height, H_{m0} (m), the energy period, T_E (s), and the mean wave direction, θ_m, (i.e. the direction associated with the principal component of the wave spectrum). Furthermore, for the model MI, an assumption of a spectral shape is required to carry out the propagation of the sea states. In this case, and based on previous wave resource assessments (Carballo, Sanchez, Ramos, Fraguela, & Iglesias 2015a), the JONSWAP wave spectrum was used (Isherwood 1987). For model MII (class 2). For model MII (class 2), 2D wave spectrum data were used with a spatial resolution of 30'. Finally, for model MIII, again space varying 2D wave spectrum data were used, but in this case they were generated from model MII, which allowed for a much higher spatial resolution (500 m) alongside the open boundaries.

With respect to the physics of the models only the source term processes (Eq. 10) that are relevant in shallow waters such as triads S_{nl3}, depth-induced wave breaking $S_{ds,b}$, and bottom friction $S_{ds,br}$, were included; whereas quadruplets S_{nl4}, whitecapping $S_{ds,w}$ and wave growth induced by wind S_{in} were turned off.

4 RESULTS

4.1 *Model validation*

In order to ensure that the models accurately predict the wave conditions in the area of study, they were validated over a period of a year (from 1st January 2014 to 31st December 2014) against hourly wave data, which was obtained from a wave buoy operated by the Irish Marine Institute in the Belmullet test site (Figure 1). The validation was carried out following the procedure explained in Section II, although only the parameters H_{m0}, T_e and J were considered. The results, expressed in percentages, are shown in Table 4:

Overall, an excellent agreement between the calculated and recommended values for the different classes was found. As expected, the results of the validation improved with the degree of refinement of the models, with MIII achieving the best results. However, for models MII and MIII, the mean systematic errors for $b(H_{m0})$ and $b(J)$ present deviations from the recommended values, especially in the case of the wave power (J). It is important to note that the values proposed by the IEC-TS are still

Table 4. Model validation results (% values).

	MI	MII	MIII
Coverage	94.47	93.89	94.09
$b(H_{m0})$	9.38	4.78	4.64
$b(T_e)$	4.41	3.98	3.56
$b(J)$	19.95	19.85	18.24
$\sigma(H_{m0})$	5.30	3.52	3.15
$\sigma(T_e)$	2.62	2.50	2.47
$\sigma(J)$	9.76	9.42	8.98

provisional and may be revisited based on the feedback of industrial projects or studies like the present one (Cornett, Baker, Toupin, Piche, & Nistor 2014).

In addition, the model was also validated following the traditional approach, comparing the time series of computed and measured wave data. Following (Neill, Lewis, Hashemi, Slater, Lawrence, & Spall 2014), the Correlation Coefficient, R, Root Mean Square Error, $RMSE$, and Scatter Index, SI, were the statistical parameters used to assess the accuracy of the model. Figure 5 show the time series of H_{m0}, T_e and J for the validation point, with the corresponding statistical analysis summarised in Table 5. The results obtained indicate again the ability of the models to accurately predict the wave conditions in the area of study (MIII shows again the best agreement), with values of the scatter index SI ($RMSE$ normalised by the mean of the observations) around 0.25 for H_{m0}, 0.13 for T_e and 0.75 for J, which confirm the good agreement observed in Figures 5.

4.2 *Annual wave resource characterisation*

Upon validation, the models were used to estimate the wave resource in the area of study. For this purpose, and following the recommendations of the IEC-TS, the model MI (Class I) was run for a period of ten years (from 01/01/2005 to 31/12/2014) with the aim of obtaining a first estimation of the areas with the largest wave energy resource over the Ireland's West coast. The mean annual spatial distribution of wave power (Figure 6), averaged over the 10 year simulation period, shows that the region presents a remarkable wave energy resource, which is homogeneously distributed with values up to 50 kWm^{-1}.

Therefore, Area I in Figure 6 (x = 416790 m, y = 6015400 m), which corresponds with the Belmullet's deep water test site, was selected to assess the wave resource in detail and to compare the performance of the three different models (MI, MII and MIII). For this purpose, the wave conditions for Area I were computed for a period of ten years (from 01/01/2005 to 31/12/2014) with a time interval of 1 hr, which translates into 87648 sea states analysed. Then, following the recommendations of the IEC-TS, the annual scatter table showing the annual number of hours of each sea state, parametrised in terms of H_{m0} and T_e, was constructed. The dimensions of each bin of the scatter table were set to 0.5 m and 0.5 s of H_{m0} and T_e, respectively, with their upper and lower bounds

Table 5. Summary of main modelling results.

		MI	MII	MIII
H_{m0}	R	0.90	0.91	0.94
	$RMSE$(m)	0.78	0.73	0.68
	SI	0.26	0.24	0.23
T_e	R	0.85	0.85	0.86
	$RMSE$(s)	1.24	1.23	1.18
	SI	0.14	0.14	0.13
J	R	0.93	0.94	0.94
	$RMSE(kWm^{-1})$	48.13	44.44	45.32
	SI	0.78	0.72	0.74

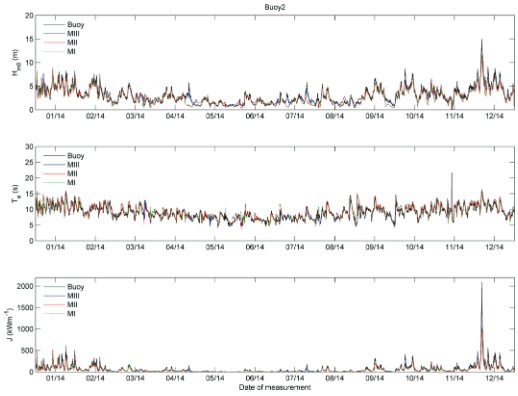

Figure 5. Time series of observed and computed wave data, H_{m01}, T_e, J.

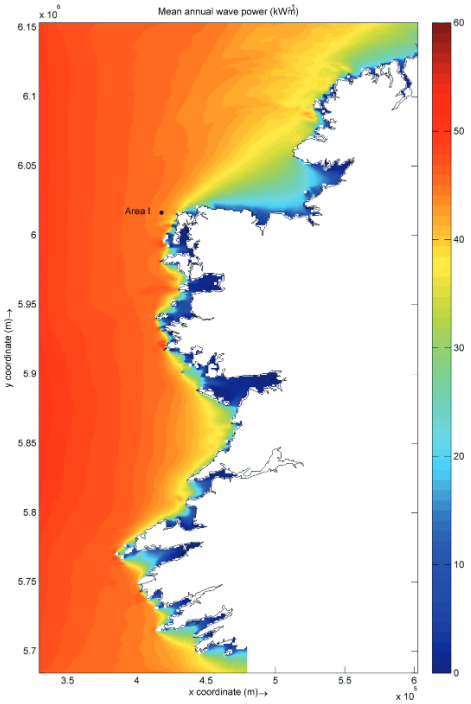

Figure 6. Annual mean wave power 2005–2014.

ensuring that a minimum of 99.9% sea states were included.

Figure 7 shows the scatter tables for Area I obtained from the three models (MI, MII and MIII). Overall, it can be observed that the total energy predicted for the models is similar, with some sea states exceeding 7 MWh^{-1}; however, MI seems to underestimate the global wave resource in comparison with MII and MIII. With respect to the distribution of the wave resource among the energy bins, considerable differences were found for the different models. For instance, in the case of MIII and MII, the maximum energy is homogeneously concentrated in the range of 3–5 m of H_{m0} and 11–12 s of T_e, whereas in MI the concentration is in 4–6 m of H_{m0} and 11–13 s of T_e, with also the presence of some very energetic sea states in the range of 6 m of H_{m0} and 13–15 s of T_e. The later is supported by the results observed in the validation section (Figures ?? and 5), where MI seems to slightly overestimate the amplitude of the variations of T_e.

In order to compare the performance of the different model classes, the absolute error for both the mean annual hours and energy of each bin was calculated. For this purpose, MIII was chosen as a reference, since it shows the best agreement with the measured data (Section 4.1). The results obtained are plotted in Figure 8. It can be observed that the differences between MI and MIII are quite significant, especially in the region of 5–6 m of H_{m0} and 12–16 s of T_e, where the differences in the estimated energy are close to the 55%. On the other hand, the differences between MII and MIII are considerably less, with only significant differences (up to 25%) concentrated in the energy bins of 7–8 m of H_{m0} and 14–15 s of T_e, which do not present an important number of annual hours. Finally, these results seem to validate the methodology proposed by the IEC-TS, highlighting the differences for each class regarding the wave resource characterisation and its distribution among the different energy bins, which can play an important role at the time of designing a wave farm.

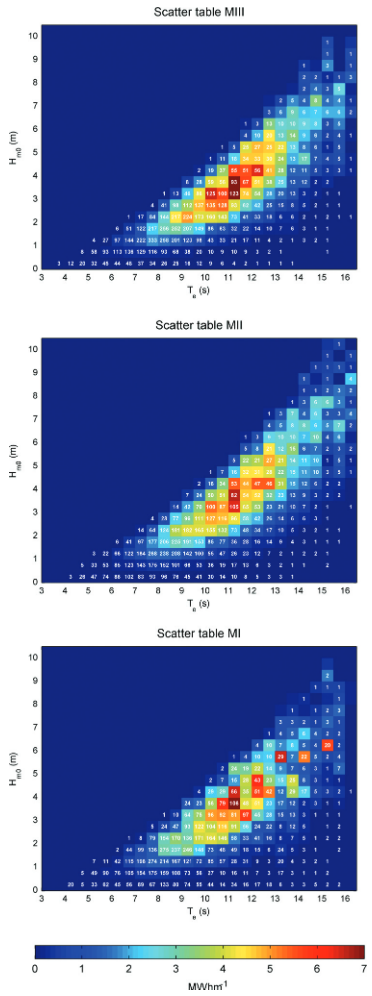

Figure 7. Scatter tables models MI, MII and MIII. Colour map (Energy ($MWhm^{1}$); Numbers (Num. annual hours energy bin).

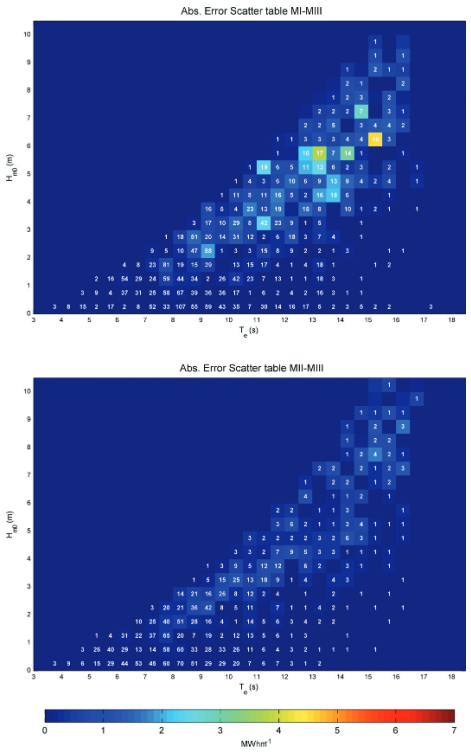

Figure 8. Absolute error between MI, MII with MIII. Colour map (Energy ($MWhm^{1}$); Numbers (Num. annual hours energy bin).

5 DISCUSSION

This section aims to offer some feedback to the IEC-TS with respect to the main aspects tackled in this investigation: the validation procedure and the wave resource characterisation. Regarding the validation procedure, it has proven to be a robust methodology, which covers a wide range of wave parameters to assess the accuracy of the model. However, there are some issues that may be addressed for future editions of the IEC-TS. First of all, in view of the results, the maximum acceptable values proposed for the weighted mean systematic error, $b(e_p)$, (Table 3) seem to be especially demanding for classes 2 and 3. As can be observed, for models MII and MIII these requirements are not met for H_{m0} and J; however, the traditional validation procedure shows an excellent agreement in both cases (Table 5 and Figures ?? and 5). Therefore, taking into account that these maximum limits are still provisional (IEC-TS is still a draft version), these limits may be increased for future editions of the IEC-TS. Of course, this also needs to be corroborated from the feedback of studies like the present one carried out in different locations (Cornett, Baker, Toupin, Piche, & Nistor 2014). Last, but not least, the IEC-TS should set clear limits regarding the size of the bins of the omni-directional scatter table for the validation procedure. For the moment, the IEC-TS has only stated that the bins should not be larger than 0.5 m and 1.0 s of H_{m0} and T_e, respectively. However, smalls modifications to the size of the bins may impact remarkably the coverage of the validation data (i.e the amount of bins that achieve minimum number of validation data points to represent the cell) and, therefore, the values obtained for the systematic $b(e_p)$ and random errors $\sigma(e_p)$. Therefore, with the purpose of clarifying and homogenising the validation procedure, IEC-TS should specifically define the size of the scatter table bins.

With respect to the methodology proposed by the IEC-TS for the wave resource characterisation, it appears to perform well for the present case study proving that the increase in the degree of refinement of the different model classes reduces drastically the level of uncertainty in the estimation of the bulk of the wave resource but also in its distribution among the different energy bins, which plays an important role when selecting the most appropriate WEC technology for a wave energy site.

Finally, the results obtained may also offer some interesting insight into the model setup process. First of all, the results for the present study show that the wave boundary conditions (parametric vs spectral boundaries) play a more important role than the mesh resolution, in relation to the accuracy of the model. As can be observed in Figures 7 and 8, the results offered by the models MII and MIII, which were set up using spectral boundary conditions, are quite similar, despite the fact the characteristics of the meshes used are completely different, mid-resolution cartesian grid vs high-resolution unstructured grid, respectively. This fact should not be considered of minor importance, especially to find the right balance between the accuracy and the computational effort required by the model, since a high-resolution model, such as MIII, requires higher computational times, whereas the level of accuracy provided is only slightly better than MII. Therefore, taking all this facts into consideration, the requirements for the Class 3 model setup regarding the minimum grid resolution may be revisited for future editions of the IEC-TS.

6 CONCLUSIONS

Over the last years, the interest in harvesting the wave energy resource has translated into a large number of wave resource assessments. Most of these studies offer a rough approximation of the wave resource, since they were carried out based on a limited number of sea states that do not cover all the energy resource over a specific coastal region. In this context, the IEC has developed a methodology (IEC-TS) with the aim of standardising the wave resource characterisation. Therefore, the aim of this work is to explore the utility of the IEC-TS by means of a case study, focusing on the validation procedure and the main aspects of the wave resource characterisation.

Overall, the IEC-TS has proven to be a robust and coherent methodology, which offers a set of recommendations and rules to carry out a precise wave resource characterisation. The validation procedure covers a wide range of parameters, with the aim of properly assessing the accuracy of the model. However, it was found that the minimum requirements needed for the validation of classes 2 and 3 may be excessively demanding and, therefore, could be subject to change for future versions of the IEC-TS. Regarding the wave resource estimation, it was found that the degree of uncertainty decreases with level of refinement of the different model classes both for the annual and intra-annual resource characterisation. From the point of view of the modelling setup, the results obtained show that the characteristics of the boundary conditions (parametric vs spectral) have a bigger impact than the grid resolution on the accuracy of the models. In addition, the grid resolution also plays an important role in the computational effort; therefore, the minimum grid resolution required for the class 3 models could be increased. Finally, it is important to point out that these recommendations should be corroborated with the feedback from other works of the same nature as the present one.

In summary, this work explores the main characteristics of the IEC-TS, although some of them

such as the seasonality of the wave resource and the wave-current interactions are outside the scope of this work and will be dealt with as a continuation of this research.

ACKNOWLEDGMENT

This research is based upon works supported by Science Foundation of Ireland under Grant No. 12/RC/2302 for the Marine Renewable Ireland (MAREI) centre. During this work V. Ramos has been supported by the I2C postdoctoral grant ED481B 2014/059-0 (Plan Galego de Investigacion Innovacion e Crecemento 2011–2015) of the Xunta de Galicia (Spain). Its authors are also indebted to the Spanish Port Authority (Puertos del Estado) for its contribution with the wave boundary data, the Irish Marine Center for providing the wave buoy data from the Belmullet test site and the Irish Centre for High-End Computing (ICHEC) for its cooperation in the computational tasks.

REFERENCES

(2014). Iec-ts 62600–101: Marine energy wave, tidal and other water current converters part 101: Wave energy resource assessment and characterisation.

Bahaj, A. S. (2011). Generating electricity from the oceans. *Renewable and Sustainable Energy Reviews 15*(7), 3399–3416.

Bento, A. R., P. Martinho, & C. G. Soares (2015). Numerical modelling of the wave energy in Galway Bay. *Renewable Energy 78*, 457–466.

Booij, N, Ris, RC, H. L. (1999). A third-generation wave model for coastal regions i. Model description and validation. *J Geophys Res C: Oceans 104*, 7649–66.

Carballo, R. & G. Iglesias (2012). A methodology to determine the power performance of wave energy converters at a particular coastal location. *Energy Conversion and Management 61*(0), 8–18.

Carballo, R. & G. Iglesias (2013). Wave farm impact based on realistic wave-wec interaction. *Energy 51*, 216–229.

Carballo, R., G. Iglesias, & A. Castro (2009). Numerical model evaluation of tidal stream energy resources in the Ria de Muros (NW Spain). *Renewable Energy 34*(6), 1517–1524.

Carballo, R., M. Sanchez, V. Ramos, J. Fraguela, & G. Iglesias (2015a). The intra-annual variability in the performance of wave energy converters: A comparative study in N Galicia (Spain). *Energy 82*(0), 138–146.

Carballo, R., M. Sanchez, V. Ramos, J. Fraguela, & G. Iglesias (2015b). Intra-annual wave resource characterization for energy exploitation: A new decision-aid tool. *Energy Conversion and Management 93*(0), 1–8.

Cornett, A., S. Baker, M. Toupin, S. Piche, & I. Nistor (International Conference on Ocean Energy (ICOE), November 4–6, 2014). Appraisal of IEC Standards for Wave and Tidal Energy Resource Assessment.

Delft University of Techonology (1993–2014). *SWAN User manual*. Delft University of Techonology.

Farrell, N., C. O. Donoghue, & K. Morrissey (2015). Quantifying the uncertainty of wave energy conversion device cost for policy appraisal: An Irish case study. *Energy Policy 78*, 62–77.

Iglesias, G. & R. Carballo (2009). Wave energy potential along the Death Coast (Spain). *Energy 34*(11), 1963–1975.

Iglesias, G. & R. Carballo (2010). Wave energy and nearshore hot spots: The case of the SE Bay of Biscay. *Renewable Energy 35*(11), 2490–2500.

Iglesias, G. & R. Carballo (2011). Choosing the site for the first wave farm in a region: A case study in the Galician Southwest (Spain). *Energy 36*(9), 5525–5531.

Iglesias, G. & R. Carballo (2014). Wave farm impact: The role of farm-to-coast distance. *Renewable Energy 69*, 375–385.

Iglesias, G., M. Lopez, R. Carballo, A. Castro, J. Fraguela, & P. Frigaard (2009). Wave energy potential in Galicia (NW Spain). *Renewable Energy 34*(11), 2323–2333.

Isherwood, R. (1987). Technical note: A revised parameterization of the jonswap spectrum. *Applied Ocean Research 9*(1), 47–50.

Lopez, M., M. Veigas, & G. Iglesias (2015). On the wave energy resource of Peru. *Energy Conversion and Management 90*(0), 34–40.

Neill, S. P. & M. R. Hashemi (2013). Wave power variability over the northwest European shelf seas. *Applied Energy 106*(0), 31–46.

Neill, S. P., M. J. Lewis, M. R. Hashemi, E. Slater, J. Lawrence, & S. A. Spall (2014). Inter-annual and inter-seasonal variability of the Orkney wave power resource. *Applied Energy 132*(0), 339–348.

Ramos, V. & G. Iglesias (2013). Performance assessment of Tidal Stream Turbines: A parametric approach. *Energy Conversion and Management 69*, 49–57.

Ramos, V., R. Carballo, M. Alvarez, M. Sanchez, & G. Iglesias (2014). A port towards energy selfsufficiency using tidal stream power. *Energy 71*, 432–444.

Rusu, L. & C. G. Soares (2012). Wave energy assessments in the azores islands. *Renewable Energy 45*, 183–196.

Silva, D., A. R. Bento, P. Martinho, & C. G. Soares (2015). High resolution local wave energy modelling in the iberian peninsula. *Energy 91*, 1099–1112.

Soares, C. G., A. R. Bento, M. Gonçalves, D. Silva, & P. Martinho (2014). Numerical evaluation of the wave energy resource along the Atlantic European coast. *Computers & Geosciences 71*, 37–49. Marine Renewable Energy.

Tiron, R., S. Gallagher, E. Gleeson, F. Dias, & R. McGrath (2015). The Future Wave Climate of Ireland: From Averages to Extremes. *Procedia {UTAM} 17*, 40–46. {IUTAM} Symposium on the Dynamics of Extreme Events Influenced by Climate Change (2013).

Veigas, M., R. Carballo, & G. Iglesias (2014). Wave and offshore wind energy on an island. *Energy for Sustainable Development 22*, 57–65. Wind Power Special Issue.

Veigas, M., M. Lopez, & G. Iglesias (2014). Assessing the optimal location for a shoreline wave energy converter. *Applied Energy 132*(0), 404–411.

der Westhuysen AJ., V. (2002). The application of the numerical wind-wave model SWAN to a selected field case on the South African Coast. *Thesis, The University of Stellenbosch, South Africa 198*, 123–45.